

A feasibility study of a triaxial cavity to determine the surface resistance of superconducting samples

E. Mahner and W. Weingarten

1. INTRODUCTION

Superconducting (sc) cavities are in operation to push the energy of the CERN LEP2 collider to energies beyond the W^\pm threshold near 80.5 GeV up to now 92 GeV per beam. They are nearly exclusively manufactured from copper with a thin niobium film inside (NbCu cavities). This technology would be even more attractive for future accelerators, if the Nb film would be better understood, in particular the slope $Q(E_a)$. Hence the desire to test sc samples of Nb and of other materials in the interesting frequency range for accelerator application (0.3 - 3 GHz).

Similar ideas have led the CEBAF (now Thomas Jefferson) laboratory to design and build a "triaxial" cavity¹. We have adopted their idea and have slightly modified their design. Details can be found elsewhere².

2. DESIGN CONSIDERATIONS

The modifications of the design were the following:

- study of sc Pb and PbSn layers on copper (to take profit of its large thermal conductivity) in order to reduce the risk of a quench;
- fixed electrical coupling in the range of low magnetic field to ease the assembly of the coupling probe and lower the risk of a magnetic field enhancement;
- possibility to dismount the sample without having to remove the cover in order to reduce the risk of contamination and to increase the turnover of sample tests. This option asks for a well defined field distribution near the joint and is based on experience on a similar design at 8 GHz³;
- cover made of low thermal conductivity metal (stainless steel with Nb coating) to increase the sensitivity of the apparatus, which is mandatory for sc coatings on copper;
- Pb gaskets instead of In, which have a tendency to glue and may create sites which emit electrons;
- possibility to study the temperature response in sub-cooled helium (as is widely used at CERN to study the LEP2 cavities);
- pumping ports attached to the outer (low field) region of the cavity to reduce the risk of contamination.

Our design of the triaxial cavity is shown in Fig. 1.

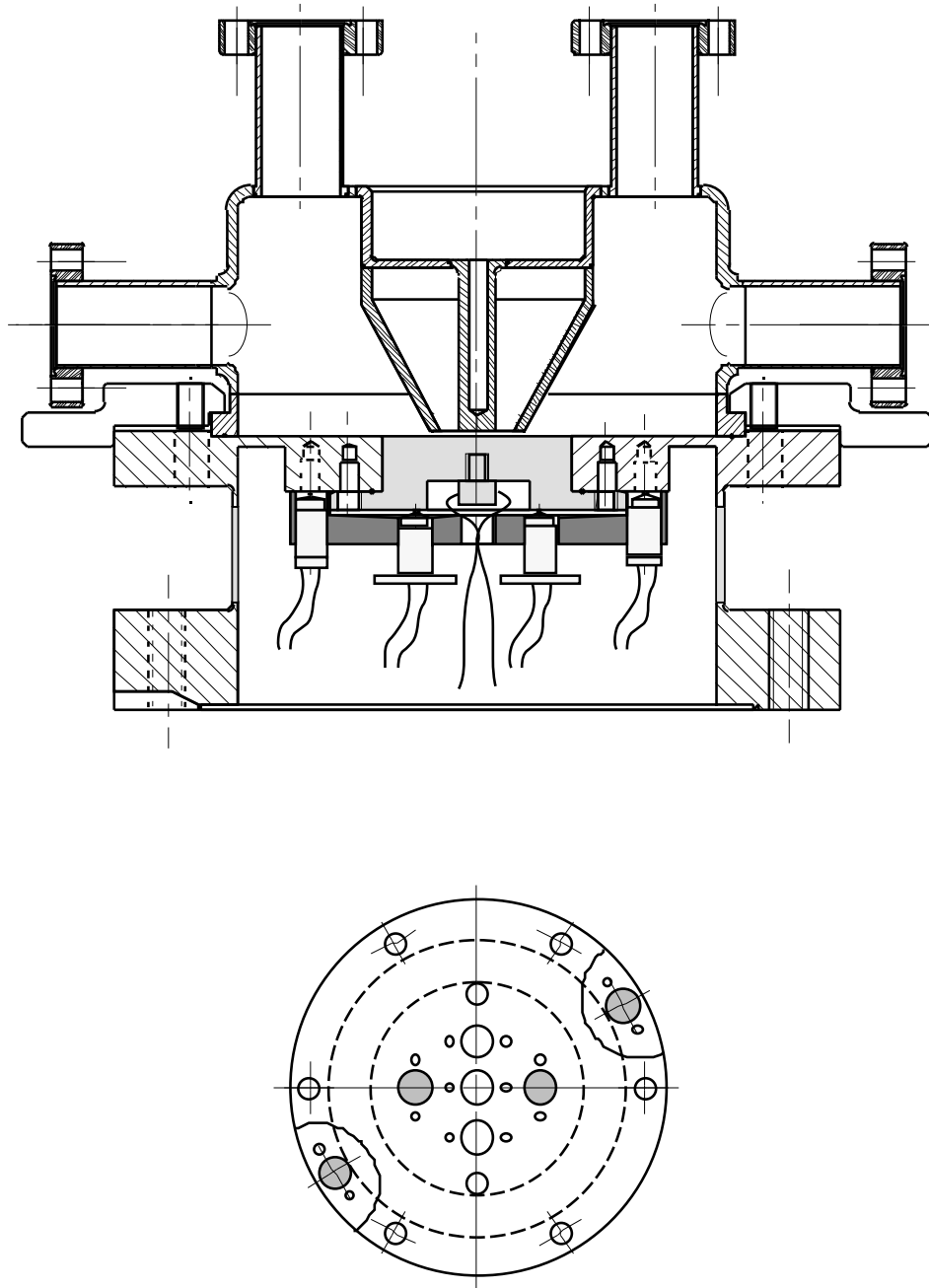


Fig. 1: Geometry of the triaxial cavity and layout of heater resistor located in the center of the sample and the temperature sensors: the thermometers (hatched circle) are arranged from left to right as T3, T1, T2, T4.

3. EXPERIMENTAL LAYOUT

After a series of exploratory tests, the most reliable layout is the one shown in Fig.

2. The main features are the following:

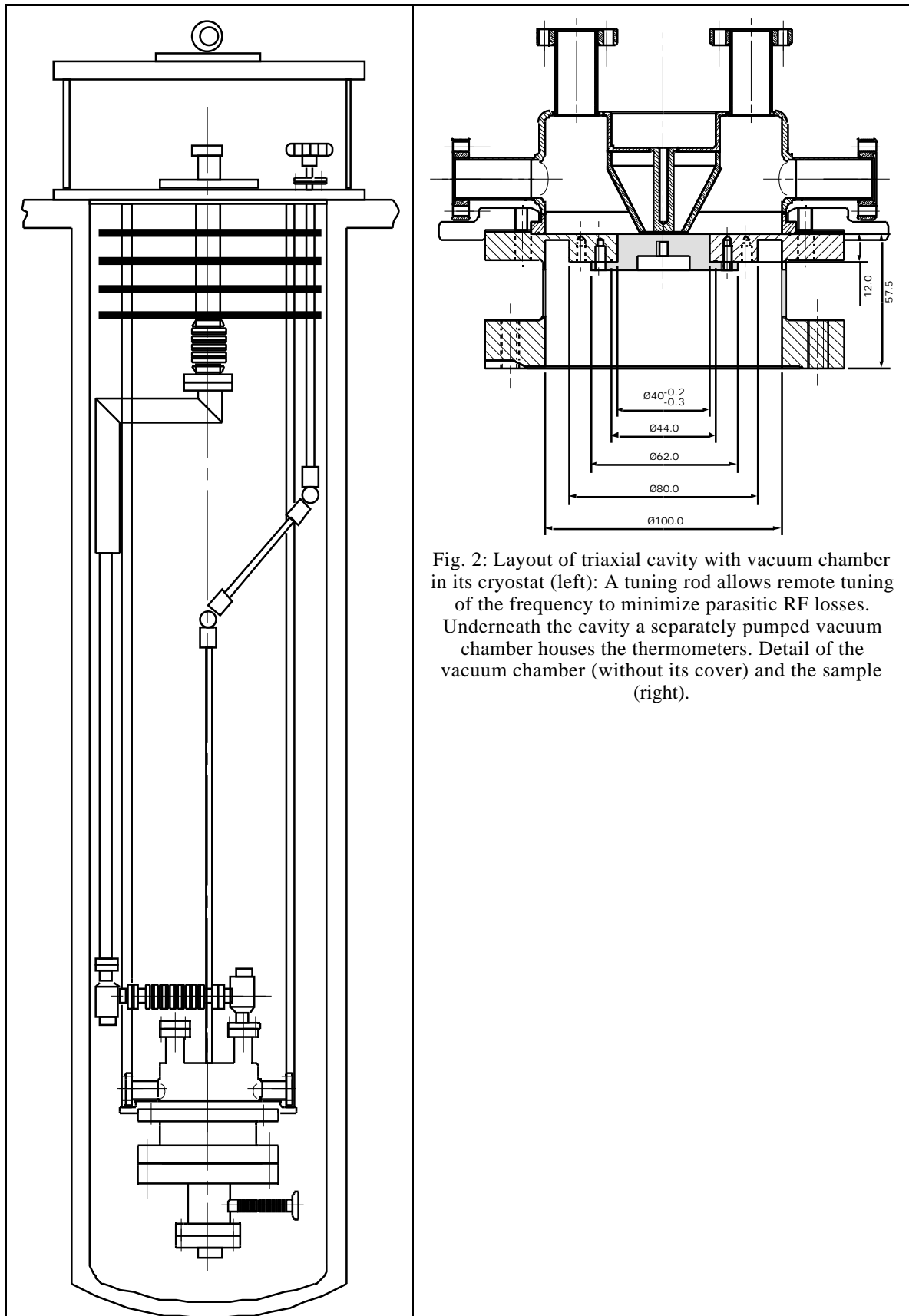


Fig. 2: Layout of triaxial cavity with vacuum chamber in its cryostat (left): A tuning rod allows remote tuning of the frequency to minimize parasitic RF losses. Underneath the cavity a separately pumped vacuum chamber houses the thermometers. Detail of the vacuum chamber (without its cover) and the sample (right).

- The cavity is in the upper position (with respect to the sample) to improve the cooling of the inner post (where the magnetic field amplitude is maximum);

- during exchange of the sample the cavity opening is directed downwards, which reduces the risk of contamination;
- a tuning rod is easily attached to the cavity (necessary to adjust the zero of the azimuthal magnetic field such that it coincides with the gap between the cover and the sample);
- the Orsay type temperature sensors⁴ give also large response both in sub-cooled and super-fluid helium.

The thermometers are calibrated between 1.8 K and 15 K by using the empirical relation between the temperature T and the resistance R , $T = V / (\lg(R) + W / \lg(R) - U)$ with three fit parameters U , V , W . The calibration may change by 50 mK at maximum for the initial cold tests, which is not harmful since we measure temperature differences. The thermometer resistance is measured by a four wire method in passing 10 μ A current and reading the voltage by means of a HP 3497a data acquisition unit.

The experiment is conducted at 4.2 K in boiling helium, for which the temperature is the most stable. It is also possible to pump down the helium bath to 1.8 K, where the pressure is controlled and stabilized by a presso-stat to within a fraction of a mbar (within hours). The cryostat with an inner diameter of 345 mm, once filled to 800 mm maximum helium level, has an autonomy of several days, also when being pumped.

The DC heater consists of a thin film C-resistor (1 k Ω , 100 mW maximum rating), which has a very small temperature coefficient. It is glued with GE varnish into the top of a copper screw, which is fixed to the sample by means of a thread. This guarantees a sufficient thermal contact. The resistor is connected to Manganin current leads of about 15 cm length each, part of which is thermally spiraled around the copper screw and fixed with a Scotch tape to provide a thermal anchor.

4. THE COMPUTER SIMULATION OF THE ELECTROMAGNETIC FIELDS INSIDE THE CAVITY

The RF parameters were calculated by means of the computer codes URMEL⁵ and SUPERFISH⁶. Important numbers are the ratio of the peak magnetic surface field on the sample B_s to that in the cavity B_p , $B_s/B_p = 25\%$, the ratio of the peak electric surface field E_p near the rim of the post to B_p , $E_p/B_p = 1.08$ ([MV/m]/mT), the geometry factor $G = 43 \Omega$, which allows to determine from the figure of merit Q_0 the average surface resistance $R_s = G/Q_0$, the ratio of the power loss on the sample P_s compared to the total power loss P_c (under the assumption of equal surface resistance), $P_s/P_c = 1.1\%$, the ratio of the power loss on the cover P_{cover} compared to the power loss on the sample

(again for equal surface resistance), $P_{\text{cover}}/P_s = 10\%$, and the ratio of B_p to the square root of the product of P_c and Q_0 (which is proportional to the stored energy),

$$\frac{B_p [\text{mT}]}{\sqrt{P_c [\text{W}] Q_0}} = 8.7 \cdot 10^{-3} \quad (1)$$

The surface resistance of the sample can be determined as follows. The ratio P_s/P_c is 0.011, provided that the average surface resistances $R_{s, \text{sample}}$ of the sample and that of the cavity, R_s , respectively, are equal. If that is not true, we obtain $P_s/P_c = 0.011 \cdot R_{s, \text{sample}}/R_s$. With Eq. 1 and $G = 43 \Omega$ we obtain

$$R_{s, \text{sample}} [\Omega] = 0.30 \cdot \frac{P_s [\text{W}]}{(B_p [\text{mT}])^2} \quad (2)$$

The zero of the magnetic field is positioned at a radius of 20 mm. This number necessitates samples with a diameter of 40 mm, which at the same time fit into general purpose thin film deposition and surface analytical equipment. The slope of this zero with a de-tuning of the resonant frequency of the cavity is $24 \mu\text{m}/\text{MHz}$, both predicted by URMEL and SUPERFISH. The magnetic field at the location of the outer joint amounts to 4 % of the maximum magnetic field on the sample and is sufficiently small.

5. COMMISSIONING OF TRIAXIAL CAVITY

5.1 Choice of cavities

Table 1: Initial performance tests of triaxial cavities

Cavity	f [MHz]	Treatment	Q [10^9] @ T [K]	Bp [mT] @ T [K]
			Bp \rightarrow 0	
CT1 (Pb/Cu)	1529	as received ¹⁾	$3.5 \pm 1.0 \cdot 10^{-3}$ @ 2.0	11.4 @ $2.0^2)$
	1527	“	$3.2 \pm 1.0 \cdot 10^{-3}$ @ 4.2	10.9 @ 4.2
CT2 (Pb/Cu)	1416	as received	$8.8 \cdot 10^{-3}$ @ 1.9	22.5 @ 1.9
	1409	“	$7.4 \cdot 10^{-3}$ @ 4.2	24 @ 4.2
CT3 (PbSn/Cu)	1434	as received	$6.0 \pm 1.0 \cdot 10^{-4}$ @ 4.2	-
CT4 (PbSn/Cu)	1468	as received	$1.0 \pm 0.1 \cdot 10^{-3}$ @ 1.8 \rightarrow 4.2	-
CT5 (Nb)	1471	CP (40), WR	0.19 @ 1.8	60 @ 1.9
	1462	“	0.037 @ 4.2	13 @ 4.2
CT6 (Nb)	1470	CP (40), WR	0.14 @ 1.9	53 @ 1.9
	1460	“	0.050 @ 4.2	13 @ 4.2

¹⁾ “As received” measured without vacuum can with a cover of identical material as the cavity.
²⁾ Several multipacting levels.

A total of six cavities was manufactured. Their initial performance was evaluated after either water rinsing (Pb/Cu and PbSn/Cu cavities) or after a standard chemical polishing (HNO_3 , H_3PO_4 , HF solution with the volume ratio 1:1:1) of 20 μm and a subsequent water rinsing (Nb cavities). The results of this initial test are summarized in Table 1.

In addition, for the Pb/Cu and the PbSn/Cu cavities, the critical temperature was also checked. It amounts to $T_c = 7.2 \pm 0.1$ K (PbSn/Cu) and to $T_c = 7.25 \pm 0.3$ K (Pb/Cu). The residual Q-values were as follows: the poorest Q-value had the PbSn/Cu cavities ($0.6 - 1.0 \cdot 10^6$), one order of magnitude larger Q-values had the Pb/Cu cavities ($4 - 9 \cdot 10^6$), and the largest Q-values had the Nb cavities ($1.4 - 1.9 \cdot 10^8$). Whereas at 4.2 K the surface resistance of the PbSn/Cu and Pb/Cu cavities was dominated by residual loss, that of the Nb cavities was close to the BCS value. The Pb/Cu cavities displayed a strong dependence of the Q-value vs. the peak surface magnetic field B_p , independent of the bath temperature down below the λ - point, the Nb cavities did not (Fig. 3).

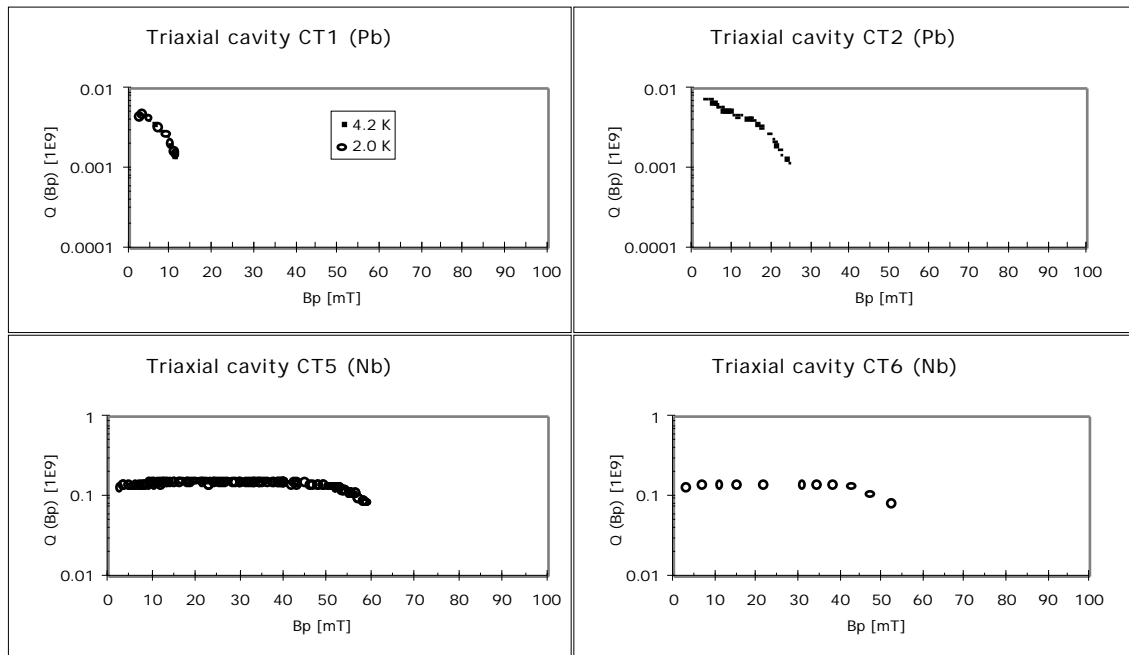


Fig. 3: Q vs. B_p curves for the Pb/Cu cavities (top) and the Nb cavities (bottom) at 1.8 K. The field in the Nb cavities is limited by electron loading.

The maximum magnetic field obtained was $B_p = 11 - 22$ mT (Pb/Cu cavities). The one for the PbSn/Cu cavities was not evaluated, because their low Q-value forbid a high field for the present coupling geometry. The Pb/Cu cavities displayed strong multipacting, which could only be passed after some hours of "RF-processing". The maximum magnetic field of the Nb cavities was 66 mT, corresponding to 71 MV/m surface electric field in the gap (Fig. 4). They did not show multipacting, but electron

loading caused by field emission. In that case, "helium processing" in pulsed mode (during about one night) usually allowed to go to the maximum fields obtained. A fast thermal quench was never observed. Some cavities could be pushed to beyond $B_p = 50$ mT without helium processing.

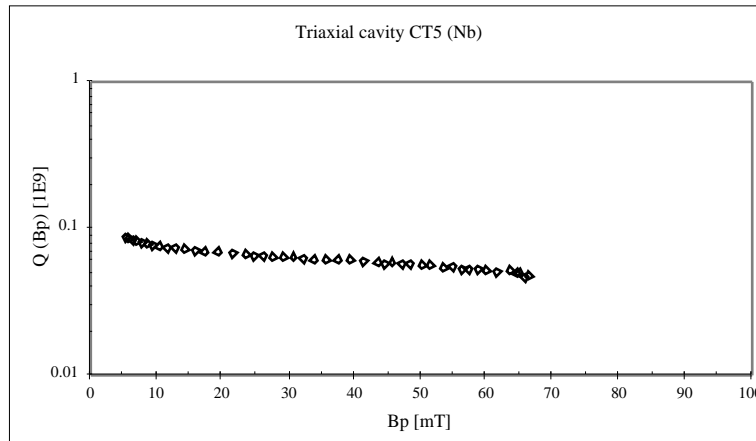


Fig. 4: Maximum surface magnetic field ever obtained during this study: $B_p = 66$ mT corresponds to a maximum surface magnetic field on the sample of $B_s = 16.5$ mT, which would correspond to 4.1 MV/m gradient in a typical sc accelerating cavity.

5.2 Choice of thermometers

a) In liquid (subcooled) helium:

The simplest layout would be such that the cover carries the sample flanged to its center hole and is immersed in liquid helium. The heat would preferentially flow perpendicularly to the surface. As is done routinely for the acceptance tests of the sc LEP cavities, thermometers located in sub-cooled liquid helium could detect the heat flow.

Such a layout was tested in a dedicated experiment: the thermometer response was calibrated vs. the RF power dissipated from a copper cylinder brazed to a copper plated stainless steel cover (Fig. 5). The temperature response follows the laws of laminar and turbulent convection cooling⁷. It allows a detection limit of 500 μ W, limited by the fluctuations of the bath temperature, which drive the convection flow. The sensitivity ranges from 2 to 5 K/W.

b) In a vacuum chamber:

A larger sensitivity and a lower detection limit is offered by housing the thermometers in a vacuum chamber (as originally done at CEBAF). Under these conditions the heat flow is directed radially outwards. The detection limit (from the voltage noise of our equipment) is 600 μ K. This solution was adopted, because it was superior to the one described under a).

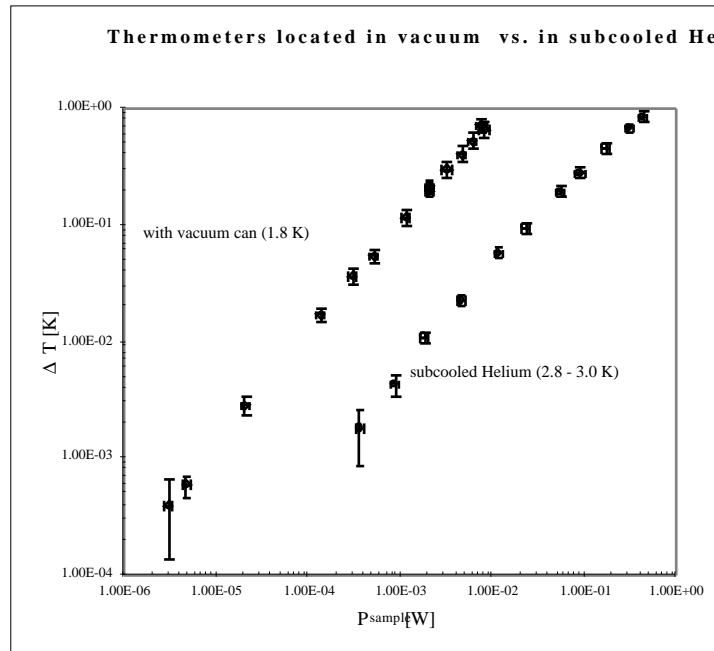


Fig. 5: Temperature response of a stainless steel cover vs. dissipated RF power. The cover is sputter coated with copper, and a copper sample (\varnothing 26 mm) is brazed to its center. Two different cooling conditions are compared (thermometers in sub-cooled helium and located inside a vacuum chamber).

5.3 Study of covers

Three types of covers were built. Cover #1 and #2 were manufactured from stainless steel in order to profit from its very low thermal conductivity. The current carrying layers of about 1 μm thickness were sputter coated with niobium, in much a similar way as the sc niobium film LEP cavities. For cover #1 the niobium was directly sputtered on the stainless steel (the most uncomplicated solution), whereas the coating for cover #2 consists of a sandwich layer of about μm thickness of the sequence stainless steel, niobium, copper, niobium. The reason was twofold: the uppermost layer was in contact with copper (and not with stainless steel), which, as we know, in principle, permits a small surface resistance. Secondly, if the layer would have peeled off, this would be clearly visible by the naked eye.

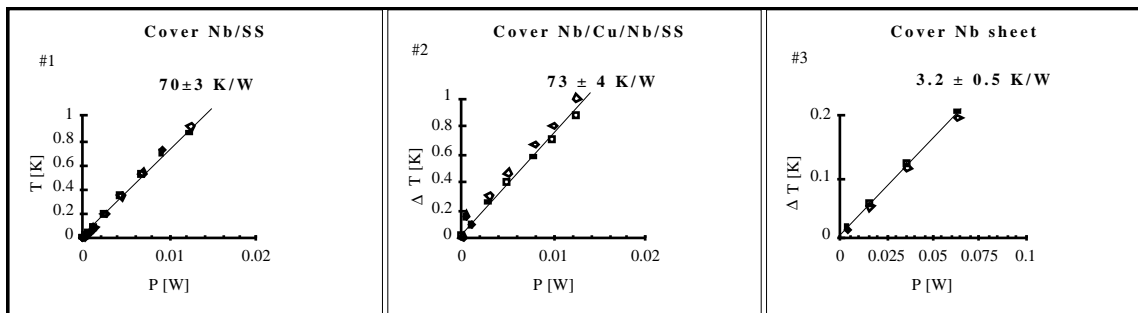


Fig. 6: Measurement of the sensitivity of the three covers: those based on stainless steel (#1 and #2) are more sensitive by about a factor of 20 than that based on niobium sheet (#3).

Cover #3 consists of low thermal conductivity niobium sheet ($RRR = 40$), with a stainless steel annulus brazed to its back. It carries the threads for the screws by which the thermometer support and the sample are fixed to the cover (Fig. 1).

As expected, the sensitivity of the three covers depends strongly on their thermal conductivity. Those made from stainless steel have a temperature response of about 70 K/W, the one made from niobium sheet has 3 K/W (Fig. 6).

The response time of the thermometers is 6 - 10 minutes. The criteria for the readout of the temperature at 4.2 K (the most stable situation) was that within one minute one thermometer at maximum out of four should deviate by 1 mK at most. At lower temperature (around 2 K), which is controlled by a presso-stat within a fraction of a mbar, we allow that two thermometers may deviate by 1 mK at most.

5.4 Parasitic losses in the joint

One specific cavity with a good RF performance was chosen for the commissioning tests (CT5, Table 3). The main result of the commissioning is the presence of RF losses (which we call parasitic losses) in between the sample and the cover, though they should ideally be impossible because the gap is located at the zero of the magnetic field. A couple of measures were undertaken to and reduce these. A 0.2 mm gap has been established between the sample and the cover to avoid any poorly defined electrical contact, the concentricity of the inner post and the conical part with respect to the sample hole has been minimized (to 50 μm) by inelastic mechanical deformation, and the minimum of the temperature response was determined by de-tuning the resonant frequency 1491 ± 1.5 MHz (Fig. 7).

The standard deviation of assembling the niobium sample with Pb (In) joint into the hole of the cover is ± 25 (30) μm .

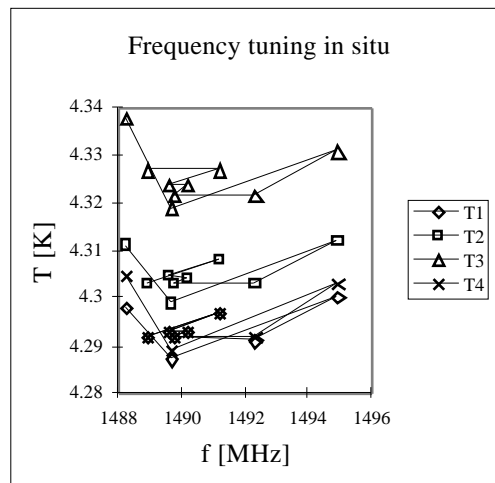


Fig. 7: In situ tuning of the resonant frequency to the value of minimum RF losses for a constant RF field amplitude: 1491 ± 1.5 MHz.

The optimum frequency of 1492 MHz can be set within a precision of less than 1 MHz by tuning the cavity to 1502 MHz at room temperature. If necessary, for instance after pumping down to 2 K, the frequency can be readjusted at low temperature within a setting precision of less than 1 MHz.

5.6 Measurement of the surface resistance of a niobium sample

A sample has been manufactured from a rod of $RRR = 40$ niobium. It was chemically polished, water rinsed, dried in a glove box and assembled to the cavity (which was water rinsed before and dried as well) in a class 100 clean room. Its surface resistance was measured in boiling helium at 4.2 and 1.8 K. The temperature of the thermometer T1 was controlled by the sample heater (within the precision mentioned in chapter 5.5) to a constant value, 4.3 K and 2.2 K, respectively. The data were plotted as shown in Fig. 8.

If the RF losses are ohmic (constant surface resistance), the sum of the heat generated in the resistor by a DC current I_{DC} and the heat generated by the RF magnetic field on the sample and elsewhere (proportional to B_p) is a constant (the total power dissipated on the sample):

$$c_1 \cdot B_p^2 + c_2 \cdot I_{DC}^2 = \text{constant} , \quad (3)$$

which gives a straight line in the $I_{DC}^2 - B_p^2$ plane.

If we measure B_p in mT, I_{DC} in A, then, with the help of Eq. 2, we identify c_1 with $R_{s, \text{ sample}}[\Omega]/0.30$, and c_2 with $1000 \Omega \cdot \gamma$, and using

$$c_1 \cdot \Delta B_p^2 + c_2 \cdot \gamma \cdot \Delta I_{DC}^2 = 0 \Rightarrow \frac{\Delta I_{DC}^2}{\Delta B_p^2} = -\frac{c_1}{c_2 \cdot \gamma} , \quad (4)$$

we obtain

$$R_{s, \text{ sample}}(B_p)[\mu\Omega] = -300 \cdot \left(\frac{\Delta I_{DC}[\text{mA}]}{\Delta B_p[\text{mT}]} \right)^2 \cdot \gamma . \quad (5)$$

The surface resistance, determined by means of Eq. 5 from the data in the top of Fig. 8, is plotted in its bottom. The error bars are understood as follows. The data points are classified in intervals according to B_p , such as 5 mT, 10 mT, 15 mT, Their length determines the error bars of B_s . Within these intervals a least square fit of $I_{DC}^2 (B_p^2)$ determines the slope and its error, by which via Eq. 5 the surface resistance and its error is calculated. Superimposed is the error of the systematic correction, which amounts to $\pm 10\%$ (cf. Table 4).

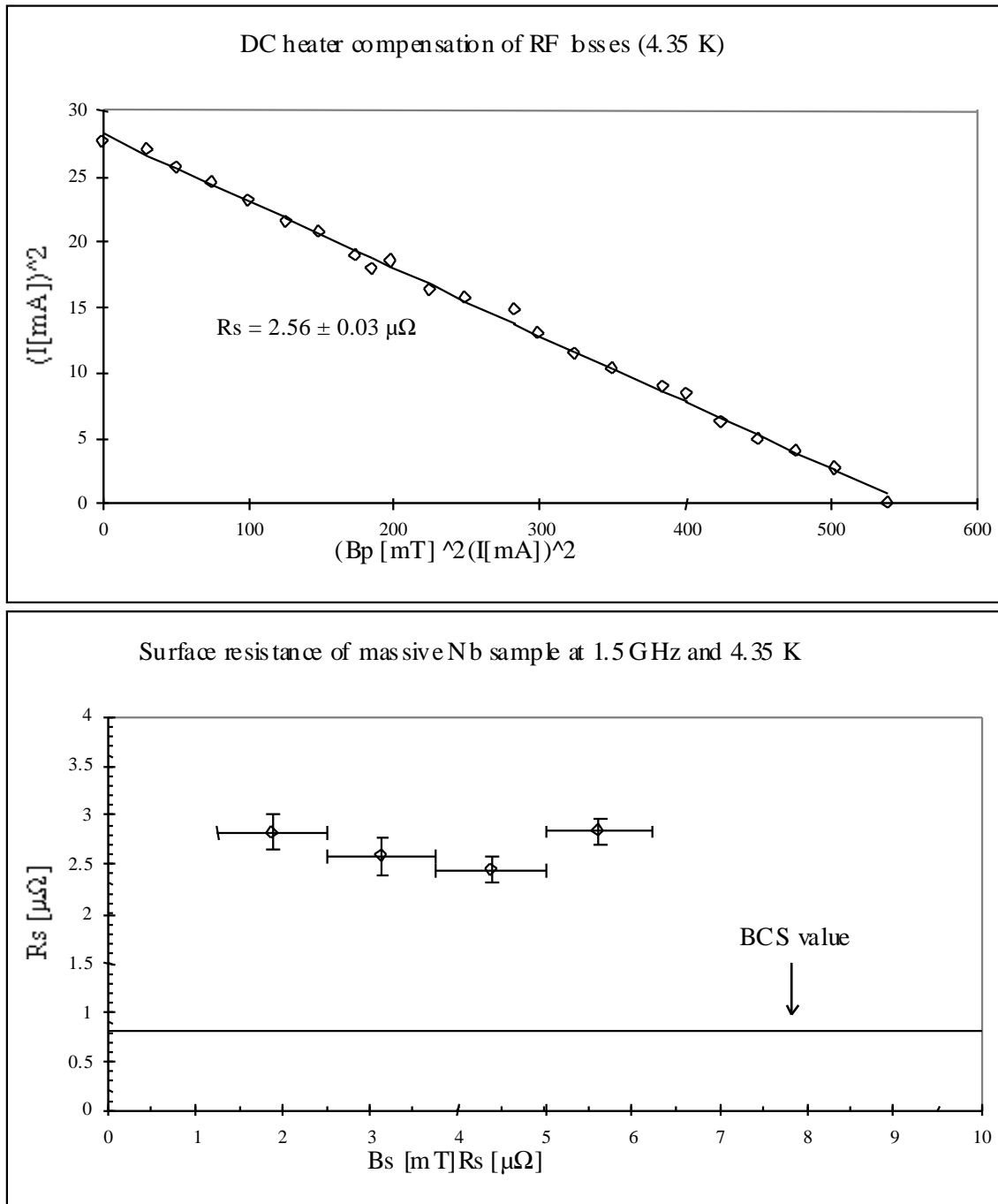


Fig. 8: Plot of B_p^2 vs. I_{DC}^2 to measure the surface resistance of a massive niobium sample at 4.35 K. The top displays the heater compensation method, the bottom shows the surface resistance vs. the magnetic field amplitude on the sample obtained from the same data. The errors indicated are statistical, systematic errors are not shown.

The surface resistance of the sample measured at 4.35 K is $2.56 \pm 0.03 \pm 0.26 \mu\Omega$. The first error is of statistical origin, the second one gives the error of the systematic correction. The BCS surface resistance is $0.8 \mu\Omega$ at 4.35 K, the average surface resistance of the cavity is $1.5 \pm 0.3 \mu\Omega$ at 4.2 K (cf. Table 3, test CT5.3.r), which corresponds to $1.7 \pm 0.3 \mu\Omega$ at 4.35 K. The discrepancy between the measured and the BCS surface

resistance can partially be attributed to the ambient magnetic field of several Gauss emanating from the stainless steel support.

6. DETECTION SENSITIVITY AND HOW TO OBTAIN A SENSITIVITY OF 1 n Ω

We define the detection limit of the surface resistance as such that the total error (which is the sum of the statistical error and the error of the systematic correction) is smaller than 10 % of the measured value. Hence, for the present layout, the detection sensitivity is limited to 2.5 $\mu\Omega$ by parasitic losses in the joint.

All elements are at hand now to determine how to obtain a detection sensitivity of 1 n Ω : the temperature detection limit of 600 μK (chapter 5.2.b)) determines for the covers #1 and #2 (with a sensitivity of 70 K/W, chapter 5.3) the minimum detectable power on the sample (9 μW). From Eq. 1, we conclude that the minimum detectable surface resistance is less than 1 n Ω , provided that the peak surface magnetic field B_p in the cavity is larger than 50 mT. This value was obtained in the cavities manufactured from niobium sheet.

We summarize the conditions that should allow a detection limit of 1 n Ω . The joint between the sample and the cover must be eliminated, hence the whole cover stands for the sample. The cover must be manufactured from stainless steel with the sample (manufactured from copper) closely and smoothly joined to it, by, for instance, brazing or electron beam welding. All surface irregularities must be removed from this joint (by machining or other techniques).

7. CONCLUSION

We have reported upon the construction and the commissioning of a series of triaxial cavities. The surface resistance R_s of a niobium sample at 4.35 K was determined to $2.6 \pm 0.3 \mu\Omega$. The major part of the error results from the uncertainty of the systematic correction. For the present layout the detection sensitivity is limited to 2.5 $\mu\Omega$ by parasitic RF losses in the joint between the sample and the cover. How to obtain a detection sensitivity of 1 n Ω is described.

ACKNOWLEDGMENTS

We like to mention the help of the following people: S. Bauer, J. Bendotti, D. Bloess, S. Calatroni, C. Dalmas, S. Forel, P. Gauss, F. Grabowski, J. P. Gris, R. Guerin, E. Haebel, M. Hauer, X. Lagrue, C. Liang, J. F. Malo, M. Marino, L. Philips, H. Preis, V. Palmieri, C. Ruivet, J. M. Rieubland, R. Russo, F. Scalambrin, F. Stivanello, R. Sundelin, and the summer students C. Dembowski, M. Koch and H. Rehfeld.

Thanks to the encouragement and help of C. Benvenuti, D. Boussard, P. Darriulat, K. Hübner and C. Wyss this project was made possible.

APPENDIX: CORRECTION OF SYSTEMATIC ERRORS DUE TO PARASITIC LOSSES IN THE COVER AND JOINT

As for nearly every calorimetric measurement, corrections are necessary to take into account systematic errors. An equivalent electrical model for visualizing the parasitic RF losses (of the cover and joint) is shown in Fig. 9. In reality the electrical currents are thermal currents, the resistances are thermal resistances and the voltages are temperatures. We make two different experiments: We measure the temperature distribution when the sample is heated by RF, and we do the same for heating by a DC heater. By measuring the temperature distribution for these two cases one may obtain an estimate of the parasitic RF losses. V_1 corresponds to the temperature measured by the thermometers T1 and T2, V_2 corresponds to that measured by T3 and T4.

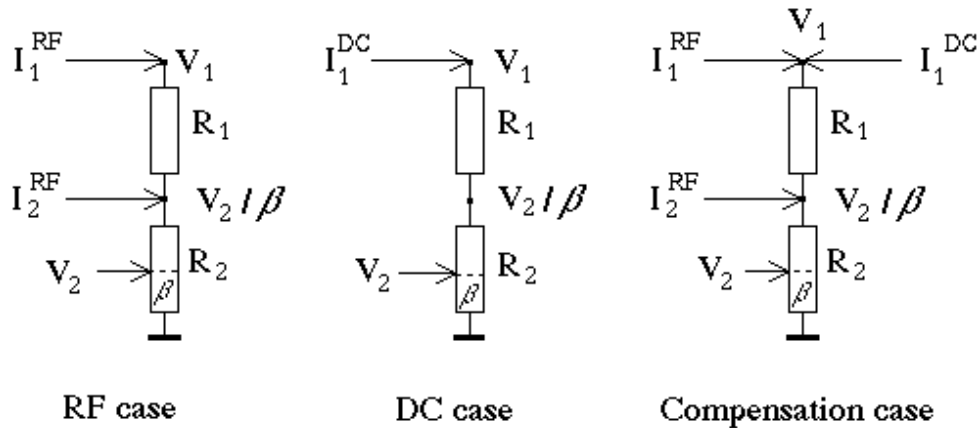


Fig. 9: Visualizing the parasitic losses

We define β as the ratio of two thermal resistances. The first one is located between the thermometers T3 and T4, and the helium bath. The second one represents the total thermal resistance between the joint and the helium bath, which cannot be measured directly. β has to be determined for instance by measuring the temperature response of a cavity the resonant frequency of which is de-tuned to the utmost such that parasitic losses in the joint will dominate the other losses. The ratio $r = R_2 / (R_1 + R_2) = \beta^{-1} (V_2/V_1)_{\text{without RF}}$ is obtained from the temperature distribution when only the DC heater is switched on, and the ratio $v = (V_2/V_1)_{\text{with RF}}$ is obtained from the temperature distribution when the RF is actuated. By defining α as the ratio of parasitic losses (I_2^{RF}) to the total losses (sum of I_1^{RF} and I_2^{RF}), $\alpha = I_2^{\text{RF}} / (I_1^{\text{RF}} + I_2^{\text{RF}})$, we obtain after some arithmetic,

$$\alpha = \frac{r\beta - v}{rv - v}$$

This constant α is a characteristic number for each sample which has been freshly mounted and has to be determined beforehand.

By applying the compensation method, we obtain for V_1 (Fig. 9)

$$V_1 = (I_1^{RF} + I_2^{RF}) \cdot R_2 + I_1^{RF} \cdot R_1 + I_1^{DC} \cdot (R_1 + R_2).$$

By controlling the temperature of the sample (represented by V_1) to a constant value, which implies $dV_1 = 0$, we end up with

$$\Delta I_1^{RF} = -\frac{1-\alpha}{1-\alpha \cdot (1-r)} \cdot \Delta I_1^{DC}.$$

On the other hand, we obtain for V_2 (Fig. 9)

$$V_2 = (I_1^{RF} + I_2^{RF} + I_1^{DC}) \cdot \beta R_2.$$

By controlling the temperature of the cover (represented by V_2) to a constant value, which implies $dV_2 = 0$, we end up with

$$\Delta I_1^{RF} = -(1-\alpha) \cdot \Delta I_1^{DC}.$$

For later use we define the ratio $\gamma = I_1^{RF} / I_1^{DC}$.

The parasitic losses give rise to a systematic error, which can in principle be corrected for. These losses were quantified (Table 4) by comparing the temperature response from a DC heater and from RF (cf. chapter 4.3). The parasitic losses are four times as large as the RF losses in the sample (for the particular test under study). In addition, it was observed that they are distributed in a non uniform manner in the azimuthal direction. The resulting correction factors γ depend very critically on β . The resulting error of γ adds up to the statistical error of the measurement (cf. chapter 5.6).

Table 4: Determination of correction factors corresponding to parasitic losses of cover #3 with Nb sample and Pb joint

	Value	Relative error [%]
v	0.96 ± 0.02	2
r	0.86 ± 0.02	2
b	0.995 ± 0.015	2
a	0.80 ± 0.025	3
$\gamma = \Delta I_1^{RF} / \Delta I_1^{DC}$	-0.23 ± 0.024	10

REFERENCES

- ¹ C. Liang et al., Rev. Sci. Instrum. 64 (1993) 1937.
- ² W. Weingarten, C. Dalmas and E. Mahner, A feasibility study of a triaxial cavity to determine the surface resistance of superconductors, SL-RF Technical Note No. 96-9.
- ³ H. Heinrichs and W. Weingarten, Nucl. Instr. Meth. 171 (1980) 185.
- ⁴ Ph. Bernard et al., Proc. 6th Workshop RF Superconductivity, CEBAF, Newport News, VA (USA), Oct. 4 - 8, 1993, p. 739; CERN AT/93 - 55 (RF).
- ⁵ T. Weiland, DESY 82-015 and DESY M-82-24.
- ⁶ K. Halbach and R. F. Holsinger, Part. Accelerators 7 (1976) 213.
- ⁷ R. Romijn et al., IEEE Trans. Magnetics MAG-19 (1983) 1318.